Available online at www.sciencedirect.com
ScienceDirect
Applied Surface Science 254 (2007) 1352–1355
applied surface science
www.elsevier.com/locate/apsusc

Analysis of the electronic configuration of the pulsed laser deposited $La_{0.7}Ca_{0.3}MnO_3$ thin films

C.N. Borca [a,*], S. Canulescu [a], F. Loviat [a], T. Lippert [a], D. Grolimund [a], M. Döbeli [b], J. Wambach [a], A. Wokaun [a]

[a] *Paul Scherrer Institut, CH-5232 Villigen, Switzerland*
[b] *Paul Scherrer Institut c/o ETH Zürich, CH-8093 Zürich, Switzerland*

Received 13 September 2007; received in revised form 18 September 2007; accepted 18 September 2007
Available online 22 September 2007

Abstract

The electronic properties of $La_{0.7}Ca_{0.3}MnO_{3-\delta}$ thin films grown by the pulsed reactive crossed beam laser ablation method are investigated. The effects of post-deposition annealing of epitaxial $La_{0.7}Ca_{0.3}MnO_{3-\delta}$ thin films have been investigated using X-ray photoelectron spectroscopy (surface sensitive) and hard X-ray absorption spectroscopy (bulk sensitive). The films deposited in the high vacuum are oxygen deficient and contain mostly Mn^{3+}. High temperature annealing in a flowing oxygen atmosphere partially changes the Mn oxidation state from +3 towards +3.4. These changes should favor a metal-like conduction and a ferromagnetic double exchange transport mechanism in the annealed thin films.

Keywords: Pulsed laser deposition; Thin films of manganates; X-ray photoemission spectroscopy; X-ray absorption spectroscopy

1. Introduction

The perovskite system $L_{1-x}A_xMnO_3$ (L, lanthanide; A, alkaline earth doping element) has been widely studied due to interesting electronic and magnetic properties [1]. The CMR effect (change in the resistivity with the applied magnetic field) observed in the lanthanum-doped compounds can be used for industrial applications, such as low field magnetic sensors or magnetoresistive reading heads [2].

The $La_{1-x}Ca_xMnO_3$ manganite materials exhibit a transition from an insulator-paramagnetic to metallic-ferromagnetic phase, with the maximum CMR effect at the transition temperature point [1]. The double exchange (DE) interaction is used as a main mechanism to explain the CMR effect. The DE interaction is related to the double exchange of e_g electrons between the Mn^{3+}–O^{2-}–Mn^{4+} network, which is possible due to the overlap between 3d orbitals of Mn species and 2p orbitals of O species. A second mechanism emphasizes the importance of polaron formation due to the Jahn–Teller effect in compounds with Mn^{3+} ions in the perovskite structure [3]. The presence of oxygen vacancies in the manganites can dramatically affect the transport properties of the materials. Moreover, when the material is processed as thin film, the crystal structure and chemical composition at the surface can have a significant influence.

In the present work, we analyze the surface composition of the $La_{0.7}Ca_{0.3}MnO_{3-\delta}$ manganite thin films using X-rays photoelectron spectroscopy (XPS) as well as the bulk electronic configuration using X-ray absorption spectroscopy (XAS) of the Mn K-edge spectra. A detailed comparison between the as-deposited and O_2 annealed thin films is performed.

2. Experimental

The $La_{0.7}Ca_{0.3}MnO_{3-\delta}$ (LCMO) thin films were grown on (1 0 0) LSAT [$(LaAlO_3)_{0.3}(Sr_2AlTaO_6)_{0.7}$] substrates, using the pulsed reactive crossed beam laser ablation (PRCLA) method [1]. A cylindrical target of LCMO with high purity (99.9%) was ablated with a KrF excimer laser (λ = 248 nm, ν = 10 Hz) using a laser fluence of 5.5 J/cm^2 and 30.000 pulses for the films growth. During the deposition process, two different oxidizing sources were used, i.e. O_2 as background gas (at a pressure of 8×10^{-2} Pa) and N_2O for the gas pulse (p = 200 kPa, duration 400 μs). The overall pressure in the chamber during the

* Corresponding author. Tel.: +41 56 310 4076; fax: +41 56 310 2688.
E-mail address: thomas.lippert@psi.ch (T. Lippert).

0169-4332/$ – see front matter
doi:10.1016/j.apsusc.2007.09.049

deposition with the gas pulse was in the range of 10^{-1} Pa. The substrate temperature was set to 650 °C during the film growth. The film thickness was measured by an Ambios Technology XP-1 profilometer. After deposition, the samples were annealed at 600 °C in a flowing oxygen atmosphere of 50 Pa O_2 for 1 and 4 h.

The XPS measurements were performed on a VG Escalab 220iXL (base pressure 5×10^{-9} Pa) instrument using monochromatic Al Kα radiation (1486.6 eV). The analyzer pass energy was set to 50 eV for survey scans and to 20 eV for narrow scans, and the energy scale was calibrated using the Ag 4d peak positions. The shifts in energy (charging) of the XPS spectra were corrected using the C 1s peak at 284.5 eV as a reference peak. The thin films were analyzed without prior surface cleaning treatment.

XANES spectra at the Mn K-edges were collected at the Swiss Light Source, at the new undulator beamline microXAS using the Si (1 1 1) double-crystal monochromator. The beam size at the sample position was 0.7 mm × 1 mm. The fluorescence mode (for thin films) as well as the transmission mode (for reference samples) has been used to acquire spectra at room temperature. The energy shifts between the various spectra were established by a careful comparison with spectra obtained from standard compounds. After background subtraction, all spectra were normalized to unity at 400 eV above the edge.

The composition of the thin films was determined using Rutherford backscattering spectrometry (RBS) and elastic recoil detection analysis (ERDA) at the PSI/ETH Laboratory for Ion Beam Physics. RBS measurements were performed using a 2 MeV ^{4}He beam and a silicon surface barrier detector under 165°. The collected RBS data are simulated using the RUMP software [4]. For the ERDA analysis a 12 MeV I^{127} beam was used under 18° incidence angle. The scattered recoils were identified by the combination of a time-of-flight spectrometer with a gas ionization chamber.

3. Results and discussions

X-ray photoemission spectroscopy analysis did not show major differences between the surface composition of the samples annealed for 1 h and the samples annealed for 4 h. Therefore, we will refer to the annealed films as samples with thermal treatment, and as-deposited films as samples without post-deposition thermal treatment. The samples thickness was around 250 nm.

The O 1s core levels, for the as-deposited and annealed films are shown in Fig. 1. The interpretation of the O 1s peaks at the manganite surface is difficult due to the presence of surface contaminants. The two O 1s peaks are influenced by the stoichiometry of the LCMO perovskite and can be assigned to contributions of the Mn-O layer, a Ca/La-O containing layer or a mixture of both [5,6]. In our case (Fig. 1), both peaks can be assigned to the perovskite structure, i.e., the peak at lower binding energy (528.7–529 eV) to the O 1s signal of the Mn-O layer, and the peak at 531 eV to the O 1s signal of the La/Ca-O layers. The peak at the higher binding energy (531.5 eV) can

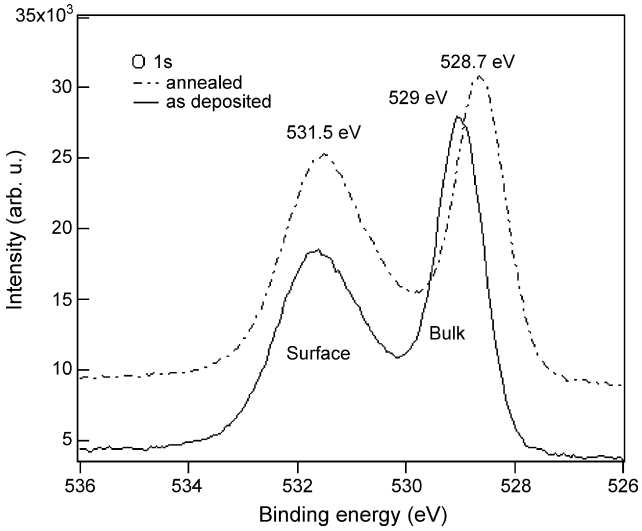

Fig. 1. XPS spectra of the O 1s peaks of the $La_{0.7}Ca_{0.3}MnO_3$ thin films.

alternatively be assigned to the presence of contaminants at the surface. Similar observations have been reported previously for $La_{0.6}Ca_{0.4}CoO_3$ thin films and have been attributed to the $CaCO_3$ surface contaminants [7]. Since the highest spectral intensity is observed for the peak at lower binding energy in Fig. 1, we assign this peak to the Mn-O surface terminal layer. A shift towards lower binding energy is observed after annealing, indicative of a more metallic character for the annealed films.

The photoelectron spectroscopy signals of the Ca 2p core levels of the perovskite structure are shown in Fig. 2. The binding energy of the Ca $2p_{3/2}$ is around 346 eV (349.26 eV for $Ca2p_{1/2}$) and shifts by 0.36 eV toward lower binding energy after annealing. The binding energy of the Ca 2p component in the $La_{0.7}Ca_{0.3}MnO_{3-\delta}$ thin films is 0.6 eV lower than that observed for $La_{0.9}Ca_{0.1}MnO_3$ [8]. The peak at 347.2 eV can be assigned to the $CaCO_3$ surface species, which is in agreement with the binding energy (BE) of the O 1s peak at 531.5 eV. The core level binding energies peaks for the as-deposited

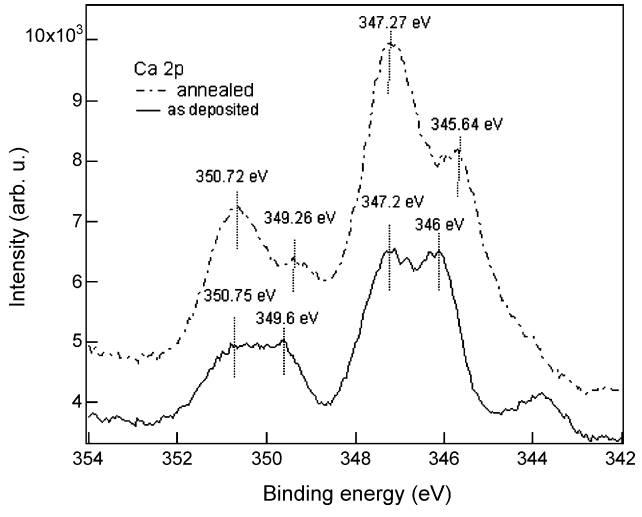

Fig. 2. Comparison of the Ca 2p peaks measured for the as-deposited and annealed $La_{0.7}Ca_{0.3}MnO_3$ films.

Table 1
Summary of the core level binding energy for as-deposited $La_{0.7}Ca_{0.3}MnO_3$ films

Material	Ca $2p_{3/2}$	La $3d_{5/2}$	O 1s
$La_{0.7}Ca_{0.3}MnO_{3-\delta}$	346.1	833.7	528.7
$La_{0.9}Ca_{0.1}MnO_3$ [8]	346.6	834.3	529.2
$LaMnO_3$ [8]	–	834.4	529.2

$La_{0.7}Ca_{0.3}MnO_3$ epitaxial films measured in this work are summarized in Table 1. For comparison, data from films of $La_{0.9}Ca_{0.1}MnO_3$ and $LaMnO_3$ are also included [8].

The XPS spectra of the La $3d_{5/2}$ peaks for the as-deposited and annealed films are shown in Fig. 3. Is it well known that the La 3d photoelectron signal exhibits a double splitting, one due to the spin-orbit interaction (named as M in Fig. 3) and an additional split due to the transfer of an electron from the oxygen ligands to the empty La 4f level (named as S in Fig. 3) [9]. The main peak (M) of the La $3d_{5/2}$ core level is located at 833.7 eV while the satellite line (S) at 838 eV. The La 3d peaks have a similar behavior as the O species, e.g. shift towards lower binding energy upon annealing.

In manganite oxide thin films, the Mn^{3+}/Mn^{4+} ratio depends strongly on the oxygen content [10]. To investigate the average Mn valence in the perovskite structure, the Mn core levels should provide the most relevant information. The Mn $2p_{3/2}$ peak is broad (not shown here) and consists of signals from the Mn^{3+} and Mn^{4+} ions, which yield peaks at different binding energies, i.e. 642.6 eV for Mn^{4+} (MnO_2) and 641.9 eV for Mn^{3+} (Mn_2O_3). A fitting of the peaks cannot be performed accurately.

It has been shown that by using the multiplet splitting values of the Mn 3s core level, the Mn average valence can be estimated quantitatively [9]. The Mn 3s core level of the transition metals exhibits an exchange splitting due to the interaction between the 3s hole created by the X-ray photoelectron emission process and 3d electrons of the Mn ion (see Fig. 4). In Table 2 the exchange splitting values,

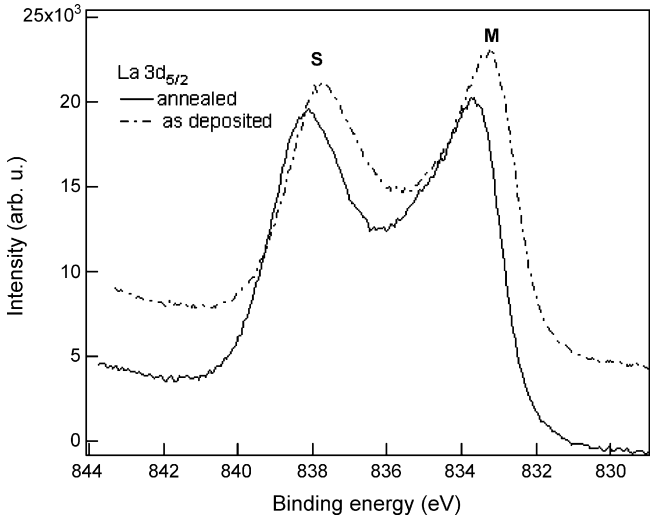

Fig. 3. The La $3d_{5/2}$ core level XPS spectra of the as-deposited and annealed $La_{0.7}Ca_{0.3}MnO_3$ films.

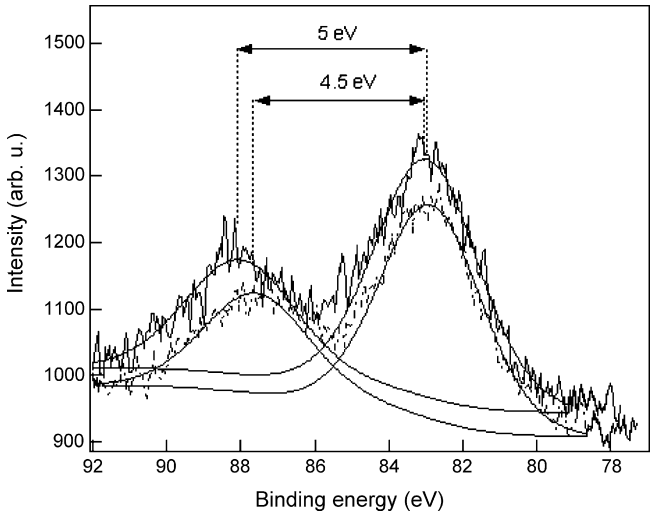

Fig. 4. Mn 3s multiplet splitting of the as-deposited $La_{0.7}Ca_{0.3}MnO_3$ films (continuous line) and annealed at 0.5 mbar O_2 atmosphere (dash–dot line) fitted with Gaussian functions.

obtained from the fitting are summarized. The films stoichiometry determined from RBS/ERDA measurements is also included, and reveals a slight increase of the oxygen content after annealing. The exchange splitting values of the reference samples, i.e., MnO_2 and Mn_2O_3 are included in Table 2.

The as-deposited samples reveal an exchange splitting of 5 eV, which is in between Mn^{3+} and Mn^{4+}, as shown in Table 2. This suggests that the Mn valence contains contributions from both Mn^{3+} and Mn^{4+} species. After annealing in oxygen atmosphere, the splitting exchange value decreases to 4.7 eV for 1 h annealing, and then decreases further to 4.5 eV for 4 h annealing. A strong oxidation of the manganites surface occurs after annealing, and therefore a layer containing Mn^{4+} species is detected at the surface. It is, therefore, important to determine if the increase in the oxidation state of the Mn species is a surface effect or also occurs in the bulk.

For the X-ray absorption measurements on the thin films only the fluorescence detection mode was employed, with an X-ray penetration depth of 8–10 μm, which samples the complete film and part of the LSAT substrate. Considering that the films have a thickness of ≈250 nm, this technique reveals therefore the bulk electronic structure. Fig. 5 shows the Mn K-edge spectra of $LaMnO_3$ and of a $SrMnO_3$ reference compounds together with the spectra for annealed (dash–dot line) and as-deposited (continuous line) $La_{0.7}Ca_{0.3}MnO_3$ thin films.

Table 2
Multiplet splitting values of the Mn 3s core level

Material	Stoichiometry (RBS/ERDA)[a]	ΔE_s (eV)
$La_{0.6}Ca_{0.4}MnO_3$ (as-deposited)	$La_{0.75}Ca_{0.25}Mn_{0.88}O_{2.75}$	5.0
$La_{0.6}Ca_{0.4}MnO_3$ (annealed)	$La_{0.75}Ca_{0.25}Mn_{0.8}O_{2.78}$	4.5
MnO_2 (Mn^{4+}) [11]		4.5
Mn_2O_3 (Mn^{3+}) [11]		5.5

[a] The systematic error is 3%.

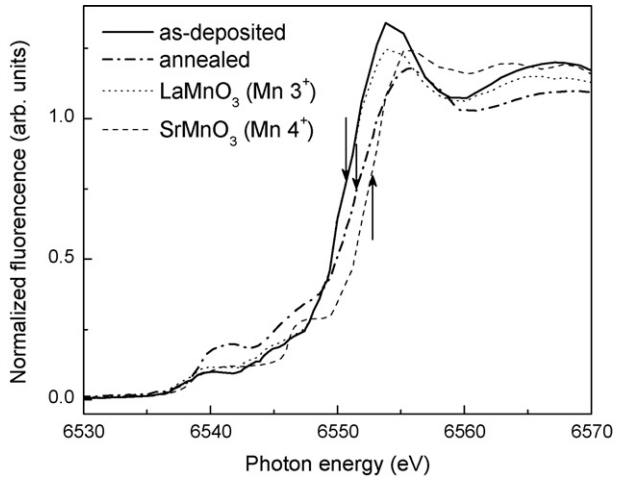

Fig. 5. Normalized Mn K main edges of $LaMnO_3$ (Mn^{3+}) (thin dotted line) and $SrMnO_3$ (Mn^{4+}) (thin dashed line) reference compounds in comparison with those of the annealed $La_{0.7}Ca_{0.3}MnO_3$ (dash–dot line) and as-deposited (continuous line) thin films. The arrows indicate the positions of the main edges.

After normalization, an energy shift of the main edge is observed, as indicated by the arrows in Fig. 5, which shows the peak position of the first derivative for the corresponding spectrum. The observed energy shift reveals that the Mn oxidation state changes from +3 in the as-deposited films to +3.4 in the annealed films. A similar energy shift was obtained previously on powder precipitates upon annealing in O_2 atmosphere and it is consistent with a Mn^{4+} t_{2g}^3 configuration [12].

The pre-edge features around 6540 eV are located approximately 15–20 eV below the main K-edge crest of manganese in Fig. 5. The pre-edge feature is related to electronic transitions from the 1s core levels to the empty 3d levels which are hybridized with 4p levels through the Mn ligands (thus, probing the density of the lowest unoccupied states). The differences in energy position and relative areas between the pre-edges of the two films can be attributed to variations in the effective number of 3d electrons in the excited-state configurations. The pre-edge area enhancement after O_2 annealing is due to an increased hybridization between the Mn d/p bands above the Fermi energy, which is supported by the increased Mn^{4+} t_{2g}^3 states.

Using two complementary electron spectroscopy techniques we were able to separate the surface-dependent (from XPS) and the bulk-dependent (from XAS) changes in oxidation states in as-deposited films and O_2 annealed films. After O_2 annealing, the surface of the films changes, containing mostly Mn^{4+} ions, while in the film bulk the presence of a mixture of Mn^{3+} and Mn^{4+} after annealing is detected, which should influence the double-exchange transport mechanism between Mn^{3+}/Mn^{4+} atom pairs. The correlation of the electronic properties with the transport and magneto-resistance properties of the thin films is currently studied in detail.

4. Conclusions

The electronic structure of $La_{0.7}Ca_{0.3}MnO_{3-\delta}$ films deposited by PRCLA was determined using XPS and XAS. The comparison between the as-deposited and O_2 annealed films shows that the Mn oxidation state changes upon post-deposition annealing. From XPS we observe an energy shift of ~0.3 eV towards lower binding energy upon annealing for all surface species, i.e. La, Ca, Mn, and O containing layers, which can be interpreted as an enhancement of the surface metallicity. An increase of the oxygen content in the LCMO thin films after annealing was detected by RBS/ERDA. And finally, from XAS, we observe a change in the Mn bulk oxidation state from +3 in the as-deposited films to +3.4 in the annealed films, suggesting that improved transport and magneto-resistance properties in the annealed films should be observed.

Acknowledgement

Financial support of the Swiss National Science Foundation is gratefully acknowledged.

References

[1] C. Martin, A. Maignan, M. Hervieu, B. Raveau, Phys. Rev. B 60 (1999) 12191.
[2] A. Malisa, Z. Ivanov, J. Magn. Magn. Mater. 295 (2005) 277.
[3] N. Mannella, A. Rosenhahn, M. Watanabe, B. Sell, A. Nambu, S. Ritchey, E. Arenholz, A. Young, Y. Tomioka, C.S. Fadley, Phys. Rev. B 71 (2005) 125117.
[4] L.R. Doolittle, Nucl. Instrum. Meth. B 15 (1986) 227.
[5] R.P. Vasquez, Phys. Rev. B 54 (1996) 14938.
[6] J. Choi, J. Zhang, S.H. Liou, P.A. Dowben, E.W. Plummer, Phys. Rev. B 59 (1999) 13453.
[7] M.J. Montenegro, M. Dobeli, T. Lippert, S. Muller, B. Schnyder, A. Weidenkaff, P.R. Willmott, A. Wokaun, Phys. Chem. Chem. Phys. 4 (2002) 2799.
[8] N.H. Batis, P. Delichere, H. Batis, Appl. Cat. A: Gen. 282 (2005) 173.
[9] E. Beyreuther, S. Grafstrom, L.M. Eng, C. Thiele, K. Dorr, Phys. Rev. B 73 (2006) 155425.
[10] I.W. Boyd, W. Zhang, Appl. Surf. Sci. 127–129 (1998) 410.
[11] V. Di Castro, G. Polzonetti, J. Electr. Spectr. Relat. Phen. 48 (1989) 117.
[12] M. Croft, D. Sills, M. Greenblatt, C. Lee, S.W. Cheong, K.V. Ramanujachary, D. Tran, Phys. Rev. B 55 (1997) 8726.